

# Low-Temperature Excitations of Dilute Lattice Spin Glasses

Stefan Boettcher\*

Physics Department, Emory University, Atlanta, Georgia 30322, USA

(Dated: February 9, 2019)

A new approach to exploring low-temperature excitations in finite-dimensional lattice spin glasses is proposed. By focusing on bond-diluted lattices just above the percolation threshold, large system sizes  $L$  can be obtained which lead to enhanced scaling regimes and more accurate exponents. This approach is demonstrated by determining the stiffness exponent for dimensions  $d = 3$  and even  $d = 6$ , the upper critical dimension. Key is the application of an exact reduction algorithm, which eliminates a large fraction of spins, so that the reduced lattices never exceed  $\sim 10^3$  variables for sizes as large as  $L = 30$  in  $d = 3$ , or  $L = 9$  in  $d = 6$ . Finite size scaling obtains  $y_3 = 0.240(5)$  for  $d = 3$ , significantly improving on previous work. The result for the upper critical dimension  $d = 6$ ,  $y_6 = 1.1(1)$ , is entirely new and compares well with a recent mean-field prediction of  $y_\infty = 1$ . PACS number(s): 05.50.+q, 64.60.Cn, 75.10.Nr.

In this Letter we propose to study low-energy excitations in Edwards-Anderson spin glasses using *bond-diluted* lattices. Any previous study of such excitations has been hampered by less-than-adequate scaling behavior that can be obtained with the limited systems sizes  $L$  accessible on undiluted lattices. Consequently, important questions regarding the spin-glass state in finite dimensional systems remain unresolved [1, 2].

A diluted lattice exhibits less frustration on short distances, and it would appear that the trade-off between potentially larger, yet less frustrated lattices should not improve the attainable scaling regime. Here, we find for the case of the ground-state stiffness [3, 4, 5] of  $\pm J$  spin glasses on diluted hyper-cubic lattices that in fact scaling corrections *diminish* for finite bond densities. Hence, in combination with finite-size scaling, a dramatically increased scaling window is obtained, leading to substantially more accurate estimates for the stiffness exponents than in previous investigations [6, 7, 8, 9].

As a further benefit, the relevant bond-density regime is located just above the percolation transition, at which diluted lattices barely exceed a mean connectivity of unity, invariably, for *any* dimension  $d$ . Accordingly, using exact graph reduction methods, we can study excitations in all dimensions with significant system sizes  $L$  that are beyond the scope of undiluted lattices. For instance, we present entirely new results for the upper critical dimension  $d = 6$ , where we can compare our results with recent mean field predictions [10]. For  $d = 4$  and 5, see Ref. [11].

Stiffness refers to the ability of a spin system in its ordered state to resist the nucleation of domains of overturned spins. The creation of such domains may entail an energetic penalty for forming an interface. The more ordered the state, the higher the energetic barrier and the more “stiff” the resistance. In turn, if the creation of such an interface is accomplished with no or reduced penalty for increasing linear size  $L$  of the domain, one may conclude that the system is in a disordered state ( $T > T_c$ ) and poses no resistance against spontaneous fluctuations spreading through the system. Thus, the

stiffness exponent  $y$  (often labeled  $\theta$ ) is a fundamental quantity to characterize the low-temperature state of a frustrated spin system [3, 12, 13], and its value is frequently relied upon [2, 14]. For instance, with the accepted value of  $y \approx 0.19$  in  $d = 3$  [6, 7], conclusions were drawn in Ref. [14] which would be excluded by the more precise value,  $y_3 = 0.240(5)$ , presented here.

The stiffness exponent is typically measured via the “defect” energy  $\Delta E$  of an interface induced in a system of size  $L$  by swapping between periodic and anti-periodic boundary conditions along one spatial direction. In a spin glass the interface of such a growing domain can take advantage of already-frustrated bonds to grow at a reduced or even vanishing cost. The width  $\sigma$  of the distribution  $P(\Delta E)$  provides a measure for the energetic cost of growing a domain of overturned spins. To wit,

$$\sigma(\Delta E) \sim L^y, \quad (1)$$

where  $L$  here refers to the size of a system with an inverted boundary condition. Clearly, it must be  $y \leq d - 1$ , and a bound of  $y \leq (d - 1)/2$  has been proposed for spin glasses generally [12]. Particularly, ground states of systems with  $y \leq 0$  are unstable with respect to spontaneous fluctuations, which can grow at no cost, like in the case of the one-dimensional ferromagnet where  $y = d - 1 = 0$ . Such a system does not manage to attain an ordered state for any finite temperature. Conversely, a positive sign for  $y$  at  $T = 0$  indicates a finite-temperature transition into an ordered regime while its value is a measure of the stability of the ordered state.

Due to its importance, there have been many attempts to approximate stiffness exponents in finite-dimensional spin glasses [4, 5, 6, 7, 8, 9, 15, 16, 17, 18], using transfer matrix, optimization, or renormalization group techniques. It has been argued long ago that  $y < 0$  for  $d \leq 2$  and  $y > 0$  for  $d \geq 3$  [4, 6]. Only recently, the stiffness exponent for  $d = 2$ , below the lower critical dimension, has been determined to considerable accuracy,  $y_2 = -0.282(2)$  [16, 17]. There has been little progress for  $d \geq 3$ , despite significant increases in computational

power. In  $d = 3$ , the accepted value so far has been  $y_3 \approx 0.19$  [6, 7], although there have been investigations recently pointing to a larger value, such as 0.23 [8] or 0.27 [16]. All of these studies are based on fitting power-laws over exceedingly narrow scaling windows at relatively small system sizes, causing large uncertainties.

We find that  $y_3 = 0.240(5)$  and  $y_6 = 1.1(1)$ . Our value in  $d = 3$  is amazingly close to (but distinct from) the Migdal-Kadanoff prediction,  $y_3^{\text{MK}} = 0.25546(3)$  [18]. Our result for the upper critical dimension  $d = 6$  suggest that recent mean-field calculations [10], which predict  $y_\infty = 1$ , have been based on valid assumptions.

To understand the shortcomings of previous investigations, it is important to appreciate the complexity of the task: Most numerical studies are based on sampling the variance  $\sigma(\Delta E)$  of the distribution of defect energies  $P(\Delta E)$  obtained via inverted boundary conditions (or variants thereof [16]). Thus, for an Ising spin glass with periodic boundaries, an instance of fixed, random bonds is generated, its ground-state energy determined, then all bonds within a hyperplane have their sign reversed and the ground-state energy is determined again. The defect energy  $\Delta E$  is the often-minute difference between those two ground state energies. Many instances of a given size  $L$  have to be generated to sample the distribution of  $\Delta E$  and its width  $\sigma(\Delta E)$  accurately. Finally,  $\sigma(\Delta E)$  has to be fitted to Eq. (1) for a sufficient range of large  $L$ .

Even small errors in the energy for either boundary condition, by way of their subtraction, may soon lead to extreme inaccuracies in  $P(\Delta E)$ . While for  $d \leq 2$  efficient algorithms exist to determine ground state energies exactly, and large system sizes can be obtained [16, 17], for  $d \geq 3$  no such algorithm exists: The minimization problem is NP-hard [19] with the cost of exact algorithms rising faster than any power of  $L$ . Hence, the values quoted previously for  $y_3$  were either based on small systems,  $L \leq 4$  [6], or on elaborate heuristic methods with  $L \leq 10$  that lead to statistical (and possibly systematic) errors [7, 8].

To overcome those limitations, we propose to increase system size  $L$  *without* increasing the optimization problem by considering reduced, bond-diluted lattices. As long as the bond density  $p$  is sufficiently above the bond-percolation threshold  $p_c$ , the dominant cluster is effectively compact so that the asymptotic scaling behavior expressed in Eq. (1) is *independent* of the degree of bond-dilution [18, 20]. Furthermore, we have developed a new, exact algorithm, that is capable of drastically reducing the size of sparsely connected spin glass systems, leaving a much reduced graph whose ground state can be approximated with great accuracy.

We will describe the reduction algorithm in more detail elsewhere [21], including its ability to compute the entropy density and overlap for sparse spin glass systems (see also [18]). We focus here exclusively on the reduction rules for the energy at  $T = 0$ . These rules apply to

general Ising spin glass Hamiltonians

$$H = - \sum_{\langle i,j \rangle} J_{i,j} x_i x_j \quad (2)$$

with *any* bond distribution  $P(J)$ , discrete or continuous, on arbitrary sparse graphs. For convenience, we use a  $\pm J$  distribution on bond-diluted hyper-cubic lattices here.

The reductions effect both spins and bonds, eliminating recursively all zero-, one-, two-, and three-connected spins. These operations eliminate and add terms to the expression for the Hamiltonian in Eq. (2), but leave it form-invariant. Offsets in the energy along the way are accounted for by a variable  $H_o$ , which is *exact* for a ground state configuration.

*Rule I:* An isolated spin can be ignored entirely.

*Rule II:* A one-connected spin  $i$  can be eliminated, since its state can always be chosen in accordance with its neighboring spin  $j$  to satisfy the bond  $J_{i,j}$ . For its energetically most favorable state we adjust  $H_o := H_o - |J_{i,j}|$  and eliminate the term  $-J_{i,j} x_i x_j$  from  $H$ .

*Rule III:* A double bond,  $J_{i,j}^{(1)}$  and  $J_{i,j}^{(2)}$ , between two vertices  $i$  and  $j$  can be combined to a single bond by setting  $J_{i,j} = J_{i,j}^{(1)} + J_{i,j}^{(2)}$  or be eliminated entirely, if the resulting bond vanishes. This operation is very useful, since it lowers the connectivity of  $i$  and  $j$  at least by one.

*Rule IV:* For a two-connected spin  $i$ , rewrite in Eq. (2)

$$\begin{aligned} x_i(J_{i,1}x_1 + J_{i,2}x_2) &\leq |J_{i,1}x_1 + J_{i,2}x_2| = J_{1,2}x_1x_2 + \Delta H, \\ J_{1,2} &= \frac{1}{2} (|J_{i,1} + J_{i,2}| - |J_{i,1} - J_{i,2}|), \\ \Delta H &= \frac{1}{2} (|J_{i,1} + J_{i,2}| + |J_{i,1} - J_{i,2}|), \end{aligned} \quad (3)$$

leaving the graph with a new bond  $J_{1,2}$  between spin 1 and 2, and acquiring an offset  $H_o := H_o - \Delta H$ .

*Rule V:* A three-connected spin  $i$  can be reduced via a “star-triangle” relation, as depicted in Fig. 1:

$$\begin{aligned} J_{i,1} x_i x_1 + J_{i,2} x_i x_2 + J_{i,3} x_i x_3 & \quad (4) \\ &\leq J_{1,2} x_1 x_2 + J_{1,3} x_1 x_3 + J_{2,3} x_2 x_3 + \Delta H, \\ J_{1,2} &= -A - B + C + D, \quad J_{1,3} = A - B + C - D, \\ J_{2,3} &= -A + B + C - D, \quad \Delta H = A + B + C + D, \\ A &= \frac{1}{4} |J_{i,1} - J_{i,2} + J_{i,3}|, \quad B = \frac{1}{4} |J_{i,1} - J_{i,2} - J_{i,3}|, \\ C &= \frac{1}{4} |J_{i,1} + J_{i,2} + J_{i,3}|, \quad D = \frac{1}{4} |J_{i,1} + J_{i,2} - J_{i,3}|. \end{aligned}$$

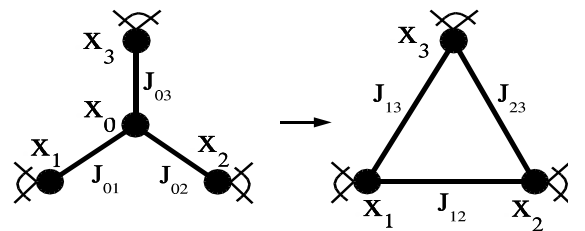


FIG. 1: “Star-triangle” relation to reduce a three-connected spin  $x_0$ . The new bonds on the right are obtained in Eq. (4).

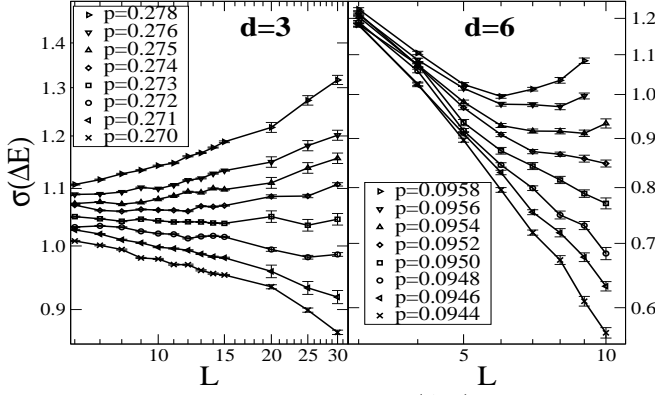


FIG. 2: Log-log plot of the variance  $\sigma(\Delta E)$  of the defect energy as a function of systems size  $L$  for various bond fractions  $p > p_c$  in  $d = 3$  (left) and  $6$  (right). At small  $p$ ,  $\sigma(\Delta E)$  drops to zero rapidly for increasing  $L$ , but turns around and rises for larger  $p$ , indicative of a nontrivial ordered state at low  $T$ . Near  $p^*$ ,  $\sigma(\Delta E)$  undergoes ever longer transients. The plots suggest  $p_{d=3}^* = 0.272(1)$  and  $p_{d=6}^* = 0.0952(2)$ .

The bounds in Eqs. (3-4) become *exact* when the remaining graph takes on its ground state. Reducing even higher-connected spins would lead to new (hyper-)bonds between more than two spins, unlike Eq. (2).

After a recursive application of these rules, the original lattice graph is either completely reduced (which is almost always the case for  $p < p_c$ ), in which case  $H_o$  provides the exact ground state energy already, or we are left with a highly reduced, compact graph in which no spin has less than four connections. We obtain the ground state of the reduced graph with the extremal optimization heuristic [22], which together with  $H_o$  provides a very accurate approximation to the ground state energy of the original diluted lattice instance.

In Ref. [20] it was shown that spin glasses with a discrete bond distribution on diluted lattices may possess a distinct critical point  $p^*$  in their bond density, which arises from the (purely topological) percolation threshold  $p_c$  of the lattice *and* the distribution of the bond weights  $P(J)$ . Clearly, no long-range correlated state can arise below  $p_c$ . A critical point distinct from percolation,  $p^* > p_c$ , emerges when such a correlated state above  $p_c$  remains suppressed due to collaborative effects between bonds [20] (see *Rule III*). Thus, to observe any glassy properties on a dilute lattice, we have to ascertain  $p > p^*$ . In Ref. [18], we were able to locate  $p^*$  for the Migdal-Kadanoff lattice, by using the defect energy scaling from Eq. (1): For all  $p > p^*$  the stiffness exponent  $y$  eventually took on its  $p = 1$  value, while for any  $p < p^*$  defect energies diminished rapidly for increasing  $L$ .

In each dimension (see Ref. [11]), we have run the above algorithm on a large number of graphs (about  $10^5 - 10^6$  for each  $L$  and  $p$ ) for  $p$  increasing from  $p_c$  in small steps. For each given  $p$ ,  $L$  increased until it was clear that  $\sigma(\Delta E)$  would either drop or rise for good. In

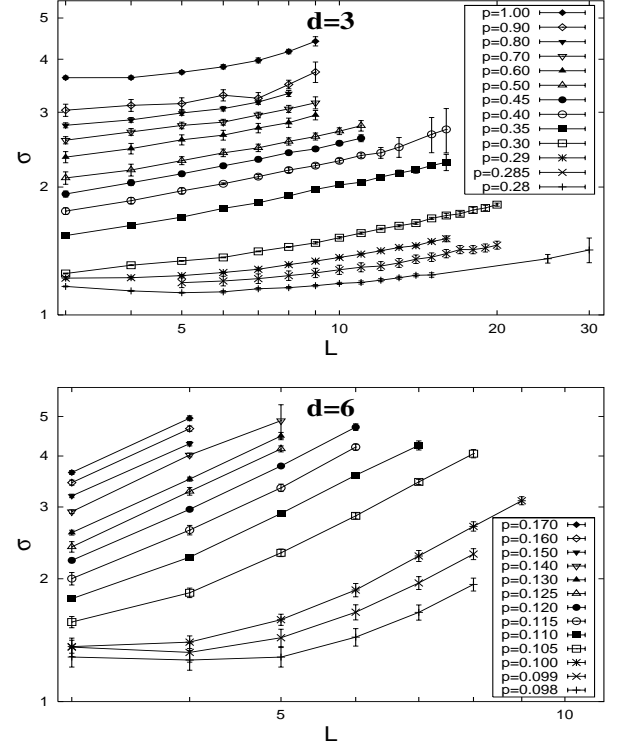


FIG. 3: Log-log plot of the width  $\sigma$  of the defect energy distribution as a function of system size  $L$  for  $d = 3$  (top) and  $6$  (bottom). The data is grouped into sets (connected by lines) parameterized by the bond density  $p$ . Most sets show a distinct scaling regime as in Eq. (1) for a range of  $L$  above finite scaling corrections but below failing heuristic accuracy.

this way, we bracket-in  $p^*$ , as shown in Figs. 2 for  $d = 3$  and  $6$ . Tab. I summarizes those results.

While the value of  $p^*$  is distribution-dependent, we merely had to establish a bond fraction beyond which we would expect Eq. (1) to hold. Then we can conduct numerical experiments to extract the asymptotic scaling of  $\sigma(\Delta E)$  for conveniently chosen  $p$ . For each choice of  $L$  and  $p$ , we have sampled the defect energy distribution with at least  $N \geq 10^5$  instances, then determined its variance  $\sigma(\Delta E)$ . For each data point for  $\sigma(\Delta E)$  we estimated its error bar as  $10/\sqrt{N}$ . In Figs. 3, we plot all the data for each dimension simply according to Eq. (1), on a logarithmic scale. For most sets of graphs, a scaling regime (linear on this scale) is visible. Yet, various deviations from scaling can be observed. Clearly, each sequence of points should exhibit some form of finite size corrections to scaling for smaller  $L$ . For large  $L$ , the inability to determine defect energies correctly, will inevitably lead to a systematic bias in  $\sigma$ . Some data sets did not exhibit any discernible scaling regime whatsoever, most notably our set for the undiluted lattice in  $d = 3$ . This may be in accordance with the observation of Refs. [23], which found very long transients in similar studies in  $d = 2$  or on undiluted Migdal-Kadanoff lattices.

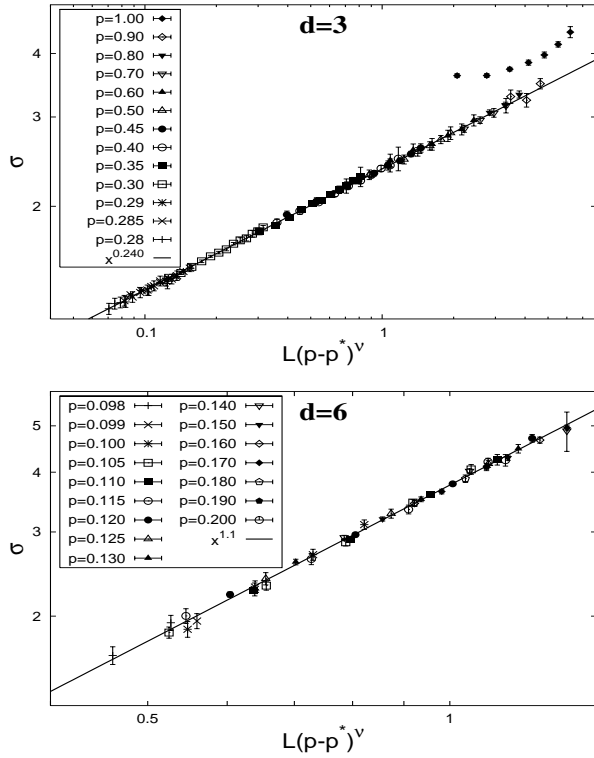


FIG. 4: Scaling plot of the data from Figs.3 for  $\sigma$ , fitted to the functional form in Eq. (5) as a function of the scaling variable  $x = L(p - p^*)^{\nu^*}$  for  $d = 3$  (top) and 6 (bottom). Data that fell outside of the scaling regime in each set of Figs. 3 was cut. The straight line in each case represents a power-law fit of the collapsed data which provides an accurate determination of the stiffness exponent  $y$  in each dimension. For  $d = 3$ , we have also included the data for  $p = 1$ , which does not appear to connect to the scaling regime.

To obtain an optimal scaling collapse of the data, we focus on the data inside the scaling regime for each set. To this end, we chose for each data set a lower cut in  $L$  by inspection. An appropriate high-end cut is introduced by eliminating all data points for which the remainder graph had a typical size of  $> 700$  spins; at that point the EO heuristic (within the supplied runtime) seems to fail in determining defect energies with sufficient accuracy. All the remaining data points for  $L$  and  $p$  are fitted to a four-parameter scaling form,

$$\sigma(\Delta E) \sim \mathcal{Y}_0 \left[ L(p - p^*)^{\nu^*} \right]^y, \quad (5)$$

suggested by Ref. [20]. Unfortunately, we have no knowledge of the functional form for finite-size corrections, making the low- $L$  cut on the data a necessity. The fitted values for the fitting constants  $\mathcal{Y}_0$ ,  $\nu^*$ , and  $y$  are listed in Tab. I. Using the parameters of this fit, we replot only the data from the scaling regime in Figs. 4.

I would like to thank the referee for suggesting the finite size scaling Ansatz, which significantly improved the presentation of the results, A. Percus and R. Palmer for

TABLE I: List of the values for the critical bond-density  $p^*$  (from Fig. 2), and the fitted values of the correlation-length exponents  $\nu^*$ , the surface tensions  $\mathcal{Y}_0$ , and the stiffness exponents  $y$ . Also listed are values for  $d = 4$  and 5 from Ref. [11].

$d$	$p^*$	$\nu^*$	$\mathcal{Y}_0$	$y$
3	0.272(1)	1.18	2.37	0.240
4	0.1655(5)	0.62	2.47	0.608
5	0.1206(2)	0.50	3.05	0.876
6	0.0952(2)	0.43	3.76	1.084

helpful discussions, and our IT staff for providing access to our student computing lab. This work was partially supported by NSF grant DMR-0312510.

\* Electronic address: sboettc@emory.edu

- [1] F. Krzakala and O.C. Martin, Phys. Rev. Lett. **85**, 3013 (2000).
- [2] M. Palassini and A.P. Young, Phys. Rev. Lett. **85**, 3017 (2000).
- [3] K.H. Fischer and J.A. Hertz, *Spin Glasses* (Cambridge University Press, Cambridge, 1991).
- [4] B.W. Southern and A.P. Young, J. Phys. C **10**, 2179 (1977).
- [5] S. Kirkpatrick, Phys. Rev. B **15**, 1533 (1977).
- [6] A.J. Bray and M.A. Moore, J. Phys. C **17**, L463 (1984).
- [7] A.K. Hartmann, Phys. Rev. E **59**, 84 (1999).
- [8] M. Palassini and A.P. Young, Phys. Rev. Lett. **83**, 5126 (1999).
- [9] A.K. Hartmann, Phys. Rev. E **60**, 5135 (1999).
- [10] T. Aspelmeier, M.A. Moore, and A.P. Young, Phys. Rev. Lett. **90**, 127202 (2003).
- [11] S. Boettcher, in preparation.
- [12] D.S. Fisher and D.A. Huse, Phys. Rev. Lett. **56**, 1601 (1986).
- [13] A.J. Bray and M.A. Moore, Phys. Rev. Lett. **58**, 57 (1987).
- [14] J.-P. Bouchaud, F. Krzakala, and O.C. Martin, *Energy exponents and corrections to scaling in Ising spin glasses*, cond-mat/0212070.
- [15] J.R. Banavar and M. Cieplak, Phys. Rev. Lett. **48**, 832 (1982); M. Cieplak and J.R. Banavar, J. Phys. A **23**, 4385 (1990); W.L. McMillan, J. Phys. C **17**, 3179 (1984).
- [16] A.C. Carter, A.J. Bray, and M.A. Moore, Phys. Rev. Lett. **88**, 077201 (2002).
- [17] A.K. Hartmann, A.J. Bray, A.C. Carter, M.A. Moore, and A.P. Young, Phys. Rev. B **66**, 224401 (2002).
- [18] S. Boettcher, Euro. Phys. J. B **33**, 439 (2003).
- [19] F. Barahona, J. Phys. A **15**, 3241 (1982).
- [20] A.J. Bray and S. Feng, Phys. Rev. B **36**, 8456 (1987).
- [21] S. Boettcher and A.G. Percus, in preparation.
- [22] S. Boettcher and A.G. Percus, Phys. Rev. Lett. **86**, 5211 (2001).
- [23] B. Drossel and M.A. Moore, Eur. Phys. J. B **21**, 589 (2001); A.K. Hartmann and M.A. Moore, Phys. Rev. Lett. **90**, 127201 (2003).